Available online at www.sciencedirect.com
SCIENCE DIRECT®
Microporous and Mesoporous Materials 81 (2005) 87–95
MICROPOROUS AND MESOPOROUS MATERIALS
www.elsevier.com/locate/micromeso

Cationic methylene blue incorporated into zeolite mordenite-Na: a single crystal X-ray study

Petra Simoncic *, Thomas Armbruster *

Laboratorium für chemische und mineralogische Kristallographie, University of Bern, Freiestrasse 3, CH-3012 Bern, Switzerland

Received 10 August 2004; accepted 19 January 2005
Available online 3 March 2005

Abstract

Single crystals of self-synthesized mordenite-Na were used for incorporation of the cationic dye molecule methylene blue (MB^+). Because the molecular size of MB^+ based on van der Waals radii (7.0×16 Å) is close to the opening of the large 12-membered ring channel of mordenite (6.5×7 Å), the molecule fits tightly into this channel. MB^+ was incorporated by ion-exchange in aqueous dye solution. The chemical composition of violet MB^+-loaded mordenite crystals was determined by an energy dispersive (EDS) element analysis yielding $Na_{5.52}MB_{0.28}Si_{42.02}Al_{5.80}O_{96} \times nH_2O$. X-ray data collection of MB^+-loaded mordenite single-crystals (MB-mordenite-Na) was performed at 120 K with synchrotron radiation ($\lambda = 0.79945$ Å) using the single-crystal diffraction line at the Swiss Norwegian Beamline, SNBL (ESRF, Grenoble) where diffracted intensities were registered with a MAR image plate. The structure of MB-mordenite-Na was refined in the monoclinic space group *Cc* converging at $R1 = 6.09\%$. Structural data of MB-mordenite-Na were compared with a structure refinement of pure mordenite-Na also measured at 120 K. Furthermore, successful incorporation of MB^+ was confirmed with optical and fluorescence microscopy. Two partly occupied molecule sites were found in the large 12-membered ring channel; one oriented upright, the other slightly inclined within the channel cross section. The tight fit of the molecule in the mordenite channel results in relatively short C···O distances from the molecule to the zeolite framework, indicating hydrogen bonding and molecule-framework interaction. The incorporation of MB^+ also influences the extra framework Na and H_2O distribution, resulting in a strongly disordered arrangement.

Keywords: Zeolite mordenite; Guest molecule; Methylene blue; Single crystal X-ray diffraction

1. Introduction

The channels and cavities of a zeolite framework provide ideal space for the incorporation, stabilization and organization of complex species as organic, luminescent dyes, metal clusters or semiconductor materials. In particular, the intercalation of luminescent dye molecules into the structure of nanoporous molecular sieves enables the design of a new kind of advanced materials, e.g. nano-scaled electronic devices, microlasers, or artificial antenna systems. Neutral as well as cationic dye molecules were successfully incorporated into various zeolites such as zeolite L, AlPO-5 and zeolite Y (see [1] for a review).

Zeolite AlPO-5 modified with the cationic dye molecule methylene blue ($C_{16}H_{18}N_3S^+$) shows nonlinear optical properties (frequency doubling, spectral hole burning) e.g. [2,3]. Furthermore, methylene blue modified zeolite Y and mordenite find potential applications for data storage e.g. [4] or chemically modified electrodes [5,6]. Furthermore, methylene blue (MB^+) organized in the channels of a zeolite shows distinct fluorescence emission explained by a Förster energy transfer mechanism

* Corresponding authors. Tel.: +41 31 631 42 72; fax: +41 31 631 39 96.
E-mail addresses: petra.simoncic@krist.unibe.ch (P. Simoncic), thomas.armbruster@krist.unibe.ch (T. Armbruster).

1387-1811/$ - see front matter © 2005 Elsevier Inc. All rights reserved.
doi:10.1016/j.micromeso.2005.01.019

[7,8]. Two different methods were established for the encapsulation of cationic methylene blue into zeolite channels, (1) the incorporation by ion-exchange in aqueous dye-solution, (2) by adding the methylene blue as a template to the zeolite-synthesis batch [9].

Several studies on MB^+ loaded zeolites have been carried out to characterize the incorporation mechanism and dye arrangement using methods such as absorption spectroscopy, X-ray photoelectron spectroscopy and X-ray powder diffraction.

Hoppe et al. reported in several studies the incorporation and characterization of methylene blue in faujasite-type zeolite and AlPO-5 [9–11]. They described the encapsulation of MB^+ by ion-exchange and crystallization inclusion and performed X-ray photoelectron spectroscopy and X-ray powder-diffraction experiments on the MB^+ modified zeolites. They showed that MB^+ is located at two different sites within the faujasite-type zeolite depending on the incorporation method.

Calzaferri et al. performed kinetics experiments on the incorporation of thionin, methylene, and ethylene blue into zeolite L [12]. They demonstrated the successful incorporation of thionin blue into the channels of zeolite L, but failed to incorporate the larger molecules methylene and ethylene blue.

An electrochemical study of MB^+ intercalated into mordenite was reported by Arvard et al. [5] and Zanjanchi and Sohrabnejad [6]. Based on diffuse reflectance spectroscopy, they reported monomeric and dimeric occurrence of methylene blue in the channels of mordenite and protonated MB^+ to MBH^{2+} by a hydration-dehydration process.

Relatively little is known about the arrangement of MB^+ molecules in the zeolite frameworks, but a detailed structural characterization focusing on a accurate localization of the dye molecule and the bonding to the zeolite framework improves the understanding of the functionality of dye-loaded zeolites.

In this study, zeolite mordenite was chosen for the structural study of incorporated cationic methylene blue. The structure of mordenite can be described as built by edge-sharing 5-membered rings of tetrahedra (secondary building unit 5-1) forming chains along the *c*-axis [13]. However, the mordenite framework can also be more comprehensibly envisioned as formed by puckered sheets parallel to (1 0 0), assembled of six-membered rings of tetrahedra [14,15]. These sheets are interlinked by four-membered rings (Fig. 1) in a way that large, ellipsoidal 12-membered (12MRc: aperture 7×6.5 Å) and strongly compressed 8-membered rings (8MRc: aperture 5.7×2.6 Å) define channels parallel to the *c*-axis. Another set of compressed 8-membered rings (8MRb: aperture 3.4×4.8 Å) connects the wide channels with the strongly compressed channels parallel to the *b*-axis.

Cationic methylene blue ($C_{16}H_{18}N_3S^+$), which was used for dye incorporation, is a sulfur-containing, single charged molecule with two methyl groups at each end of the molecule and a molecular size of 16×7.0 Å based on van der Waals radii [9] (Fig. 2).

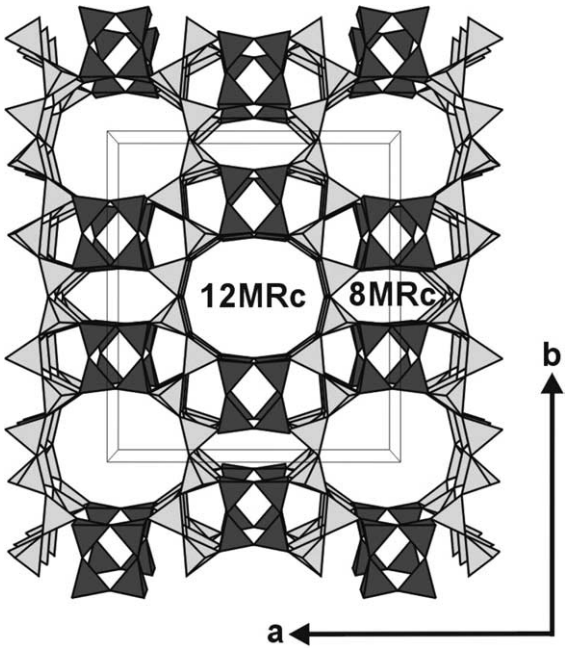

Fig. 1. Tetrahedral framework structure of mordenite with unit-cell outlines. The structure can be envisioned as built by puckered sheets (light gray shading) parallel to (1 0 0) formed by six-membered rings of tetrahedra. These sheets are connected along *a* by 4-membered ring pillars (dark gray shading) in a way that 12-membered ring channels (12MRc) and compressed 8-membered ring channels (8MRc) are formed, both extending along *c*.

The aims of this study are: (1) Incorporation of MB^+ in self-synthesized, large mordenite single-crystals; (2) study of location and bonding of MB^+ in mordenite channels by single-crystal X-ray diffraction.

The combination of the relatively low symmetry of mordenite (pseudo-orthorhombic) with the oblate cross-section of the channels suggested a more anisotropic orientation of the molecule compared to hexago-

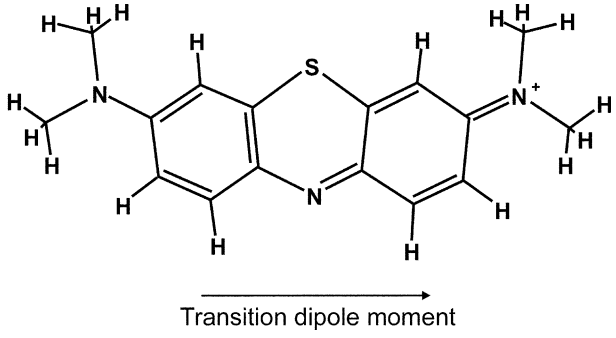

Fig. 2. Cationic methylene blue molecule ($C_{16}H_{18}N_3S^+$). The organic molecule (7.0×16 Å) fits into the large 12-membered ring channel of mordenite. Black arrow indicates the direction of the transition dipole moment.

nal or cubic zeolites, such as zeolite L or Y. The arrangement of dye molecules incorporated in the channels of zeolite L or Y exhibits usually pronounced disorder caused by the high symmetry of tetrahedral framework [11,16,17]. Because the molecular size of MB^+ based on van der Waals radii (7.0×16 Å) is close to the pore opening of the large 12-membered ring channel of mordenite (7×6.5 Å), the molecule fits tightly into the channel. This tight fit limits rotational disorder within the channel and simplifies the accurate localization of the molecule and characterization of molecule-framework interactions.

2. Experimental

Pure mordenite-Na single crystals for subsequent dye incorporation and X-ray diffraction experiments were hydrothermally synthesized after a modified method of Warzywoda et al. [18]. This method uses preheated silica gel (Aldrich) and sodium aluminate (Riedel de Haen) as starting materials, which are dissolved in NaOH solution with the addition of a small amount of ethanol. Synthesis conditions were reported in detail elsewhere [19]. Synthesis products were 100% mordenite-Na with platy morphology and an average size of $0.05 \times 0.05 \times 0.06$ mm. The crystals were examined with a scanning electron microscope and showed no twinning but slightly curved faces.

The self-synthesized mordenite-Na was used for encapsulation of cationic methylene blue (MB^+). The accessibility of the large 12-membered ring channels of the mordenite framework was demonstrated by previous incorporation experiments with elemental selenium [20] and cationic thionin blue [21]. Dye incorporation was carried out by ion exchange in an aqueous solution. Pure mordenite-Na single crystals (0.5 g) were treated in 8×10^{-3} M aqueous methylene blue trihydrate solution ($C_{16}H_{18}ClN_3S \times 3H_2O$, Aldrich) at 90 °C for 12 weeks in a sealed Teflon vessel. The dye solution was renewed every week. After ion exchange, crystals were extensively washed with hot distilled water and ethanol to remove adsorbed molecules from the crystal surface. The chemical composition of MB^+-loaded mordenite was determined by energy-dispersive (EDS) element analysis using a scanning electron microscope yielding $Na_{5.52}MB_{0.28}Si_{42.02}Al_{5.80}O_{96} \times nH_2O$, where the S-concentration was taken as measure of the MB^+ content.

Furthermore the incorporation of MB^+ was confirmed by optical microscopy and fluorescence microscopy. MB^+ loaded mordenite single-crystals were investigated with plane-polarized light using an optical microscope. Crystals were investigated in two settings: (1) incident beam perpendicular to the (0 0 1) face; (2) incident beam perpendicular to the (1 0 0) face. In setting (1), the crystal is violet, if the polarization direction is parallel to the *a*-axis. The crystal appears only light violet to nearly colorless with a polarization direction parallel to the *b*-axis. In setting (2), the crystal appears dark, nearly black with a polarization direction parallel to the *c*-axis. On the other hand, the crystal appears light violet to nearly colorless with a polarization direction parallel to the *b*-axis. These pleochroism phenomena reflect the anisotropic arrangement with a relatively limited spreading of the molecules within the channel cross-section and can be explained by the orientation of the molecule's transition dipole moment, which runs along the molecule's long axis. The strong absorption (setting (1) parallel to the *a*-axis, setting (2) parallel to the *c*-axis) indicates a transition dipole moment nearly parallel to the polarization direction, whereas the weak absorption (setting (1) parallel to the *b*-axis, setting (2) parallel to *b*-axis) points to a nearly perpendicular orientation of the transition dipole moment to the polarization direction. Non-polarized fluorescence microscopy of the MB^+ loaded mordenite crystals using a wavelength of 545–580 nm results in intense emission of red light caused by the excitated MB^+ molecules.

X-ray data collection of synthetic mordenite-Na (as synthesized) and methylene blue-treated (MB-mordenite-Na) single crystals were performed at 120 K using a conventional N_2 gas cooling device (Oxford cryosystems) and synchrotron radiation (wavelength $\lambda = 0.79946$ Å) on the single-crystal diffraction line at SNBL (ESRF, Grenoble). The diffracted intensities were registered with a MAR image plate. The double experiments were performed to detect possible phase transitions in the mordenite structure at low temperature due to the influence of the incorporation of the dye molecule. The reason for intensity data collection at low temperature was to reduce thermal vibration and disorder of the extra framework dye molecules in order to allow more accurate localization. Data reduction was performed with the program package CrysAlis [22] and an empirical absorption correction was made with Sadabs [23]. A summary of experimental parameters is given in Table 1.

Structure refinement for mordenite-Na and MB-mordenite-Na was carried out with the program SHELXL97 [24], using neutral-atom scattering factors (Si for all tetrahedral sites—labeled T sites). Refinements were performed with anisotropic displacement parameters for all framework sites. The mordenite structure at room temperature is usually refined in space group *Cmcm* [13] or $Cmc2_1$ [25], respectively. Simoncic and Armbruster [19] proposed a domain like structure where about 3% of the Si/Al framework is shifted by *c*/2. In spite of these studies, the symmetry of the framework is generally handled as pseudo symmetry and represents only a fair approximation. Lower symmetries or micro-twin models are also supposed [26] but not proven by experiments. As already shown in the structure refinement of pure mordenite-Na and selenium-modified mordenite-Na at 120 K [20], the monoclinic space group

Table 1
Experimental parameters for X-ray data collection and refinement of mordenite-Na and MB-mordenite-Na

Sample	Mordenite-Na	MB-mordenite-Na
Crystal size (mm)	$0.05 \times 0.04 \times 0.05$	$0.06 \times 0.04 \times 0.05$
Diffractometer	MAR image plate	MAR image plate
X-ray radiation	Synchrotron (0.7995 Å)	Synchrotron (0.7995 Å)
Temperature	120 K	120 K
Space group	*Cc*	*Cc*
Cell dimensions (Å)	18.073(3), 20.463(3), 7.5145(9)	18.159(4), 20.349(4), 7.492(1)
β (°)	90.05(1)	90.03(1)
Absorption corr.	Sadabs	Sadabs
Maximum 2θ	55.13	55.12
Measured reflections	15595	15404
Index range	$-20 \leqslant h \leqslant 20$, $-23 \leqslant k \leqslant 23$, $-8 \leqslant l \leqslant 8$	$-20 \leqslant h \leqslant 20$, $-23 \leqslant k \leqslant 23$, $-8 \leqslant l \leqslant 8$
Unique reflections	4468	4390
Reflections > $4\sigma(F_0)$	4180	4226
R_{int}	0.0347	0.0479
R_σ	0.0398	0.0444
Number of l.s. parameters	362	392
GooF	1.131	1.116
$R1$, $F_0 > 4\sigma(F_0)$	0.0525	0.0609
$R1$, all data	0.0573	0.0630
w$R2$ (on F_0^2)	0.1095	0.1576

Cc was used as a "best fit" for the agreement between structure model and diffraction data of MB^+ loaded mordenite. Final data for MB-mordenite-Na are therefore presented in monoclinic space group *Cc*. In addition, a *c*/2-shifted defect domain was introduced and fully constrained to the Si/Al framework. To reduce correlation problems due to pseudo symmetry, related tetrahedral sites were constrained to each other. Na- and H_2O positions were determined by comparison with diffraction data of synthetic mordenite-Na at room temperature [19] and 120 K [20], analyzing interatomic distances and difference Fourier maps.

MB^+-molecule sites were determined analyzing the difference Fourier map focusing on the large 12-membered ring channel, and in comparison with the electron density within the 12-membered ring channel of the pure mordenite-Na. Two partly occupied MB^+ molecule sites were found. One site (molecule 1) is oriented nearly upright within the large 12-membered ring channel, whereas the other site (molecule 2) is slightly inclined within the channel cross-section (Fig. 3). Because the electron density peaks within the 12-membered ring channel indicated distinct disorder, the nearest neighbor and next nearest neighbor distances within the molecule were fixed during the refinement using bond lengths reported for methylene blue [27], and optimized with ChemSketch structure package [28]. S-C nearest neighbor distances were fixed to 1.73–1.74 Å, C–C distances to 1.35–1.49 Å, and N–C distances to 1.30–1.40 Å. The population of individual atoms was constrained to be equal for both molecules. Isotropic displacement parameters of S-, C- and N-atoms were fixed. All molecules were constrained to flat geometry, whereas the H-atoms are not included in the refinement.

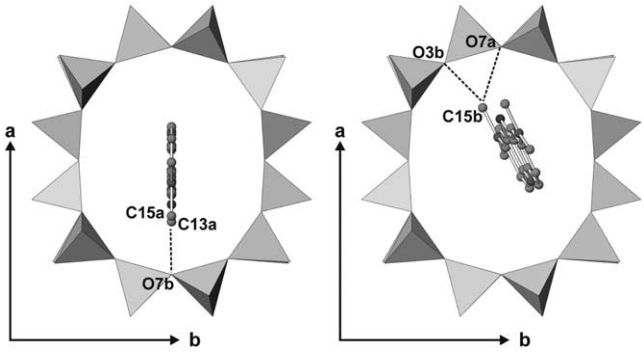

Fig. 3. MB^+ molecule sites within the large 12-membered ring channel down *c*. Shortest C···O distances from the molecules to the channel wall oxygens are indicated by dashed lines. H-atoms are not displayed.

More details about the refinement of the Si, Al framework of mordenite-Na at 120 K can be found in Simoncic and Armbruster [20].

3. Results and discussion

The results of the structure refinement for MB-mordenite-Na, including atomic coordinates, populations, and isotropic displacement parameters are given in Table 2. Detailed structural data as atomic coordinates of mordenite-Na, and tetrahedral T–O bond lengths and anisotropic displacement parameters of mordenite-Na and MB-mordenite-Na can be found in [29].

In comparison with the unit cell of mordenite-Na (Table 1), the unit cell dimensions of MB-mordenite-Na show a significant expansion along the *a*-axis and a shorting along the *b*-axis. The entering of the large

Table 2
Atomic coordinates and B_{eq} values for dye-loaded MB-mordenite-Na (space group *Cc*)[1–27]

Atom	Population	*x*	*y*	*z*	B_{eq} (Å^2)
T1a	0.969(1)	0.30378(4)[1]	0.07350(3)[2]	0.1684(3)[3]	1.12(4)
T1b	0.969(1)	0.30378(4)[1]	−0.07350(3)[2]	0.0842(1)[4]	0.93(3)
T1c	0.969(1)	−0.30378(4)[1]	0.07350(3)[2]	0.1684(3)[3]	1.66(5)
T1d	0.969(1)	−0.30378(4)[1]	−0.07350(3)[2]	0.0842(1)[4]	1.33(4)
T2a	0.969(1)	0.19674(4)[5]	0.19025(3)[6]	0.6668(2)	1.23(4)
T2b	0.969(1)	0.19674(4)[5]	0.19025(3)[6]	0.0780(2)[7]	1.14(5)
T2c	0.969(1)	−0.19674(4)[5]	0.19025(3)[6]	−0.3334(1)	1.18(4)
T2d	0.969(1)	−0.19674(4)[5]	0.19025(3)[6]	0.0780(2)[7]	1.08(4)
T3a	0.969(1)	0.41414(5)[8]	−0.11949(5)[9]	0.3776(4)[10]	1.09(4)
T3b	0.969(1)	−0.41414(5)[8]	−0.11949(5)[9]	0.3776(4)[10]	1.14(4)
T4a	0.969(1)	0.08524(5)[11]	0.22445(5)[12]	0.3721(4)[13]	1.18(4)
T4b	0.969(1)	−0.08524(5)[11]	0.22445(5)[12]	0.3721(4)[13]	1.03(4)
O1a	0.969(1)	0.3764(1)[14]	−0.0893(1)[15]	0.199(1)	3.8(2)
O1b	0.969(1)	0.3764(1)[14]	−0.0893(1)[15]	0.5525(9)	3.7(2)
O1c	0.969(1)	−0.3764(1)[14]	−0.0893(1)[15]	0.1989(9)	3.3(1)
O1d	0.969(1)	−0.3764(1)[14]	−0.0893(1)[15]	0.552(1)	3.3(1)
O2a	0.969(1)	0.1228(1)[16]	0.1941(1)[17]	0.195(1)	3.1(2)
O2b	0.969(1)	0.1228(1)[16]	0.1941(1)[17]	0.541(1)	2.4(1)
O2c	0.969(1)	−0.1228(1)[16]	0.1941(1)[17]	0.186(1)	3.4(2)
O2d	0.969(1)	−0.1228(1)[16]	0.1941(1)[17]	0.549(1)	3.3(2)
O3a	0.969(1)	0.2366(1)[18]	0.1221(1)[19]	0.640(1)	3.2(1)
O3b	0.969(1)	0.2366(1)[18]	0.1221(1)[19]	0.126(1)	3.2(1)
O3c	0.969(1)	−0.2366(1)[18]	−0.1221(1)[19]	0.621(1)	4.2(1)
O3d	0.969(1)	−0.2366(1)[18]	−0.1221(1)[19]	0.144(1)	4.2(1)
O4a	0.969(1)	−0.4066(2)[20]	−0.1977(2)[21]	0.377(2)[22]	4.4(1)
O4b	0.969(1)	0.4066(2)[20]	−0.1977(2)[21]	0.377(2)[22]	4.4(1)
O5a	0.969(1)	0.1736(4)	0.1930(3)	0.8736(9)	2.4(2)
O5b	0.969(1)	−0.1683(4)	0.1938(4)	−0.127(1)	3.6(2)
O6a	0.969(1)	0.3262(2)[23]	0.0811(1)[24]	0.3803(8)[25]	2.24(5)
O6b	0.969(1)	−0.3262(2)[23]	0.0811(1)[24]	0.3803(8)[25]	2.24(5)
O7a	0.969(1)	0.2755(4)	0.0003(3)[26]	0.1279(9)[27]	2.31(5)
O7b	0.969(1)	−0.2749(4)	0.0003(3)[26]	0.1279(9)[27]	2.31(5)
O8a	0.969(1)	0.2557(4)	0.2430(3)	0.1445(9)	2.0(1)
O8b	0.969(1)	−0.2481(5)	−0.2530(5)	0.613(1)	3.2(1)
O9	0.969(1)	−0.5029(4)	−0.0976(2)	0.369(1)	2.31(5)
O10	0.969(1)	0.0012(5)	0.2011(2)	0.375(1)	2.31(5)
T1Ba	0.031(1)	−0.30378(4)	−0.07350(3)	0.1684(3)	2.37*
T1Bb	0.031(1)	−0.30378(4)	0.07350(3)	0.0842(1)	2.37*
T1Bc	0.031(1)	0.30378(4)	−0.07350(3)	0.1684(3)	2.37*
T1Bd	0.031(1)	0.30378(4)	0.07350(3)	0.0842(1)	2.37*
T2Ba	0.031(1)	−0.19674(4)	−0.19025(3)	0.6668(2)	2.37*
T2Bb	0.031(1)	−0.19674(4)	−0.19025(3)	0.0780(2)	2.37*
T2Bc	0.031(1)	0.19674(4)	−0.19025(3)	−0.3334(1)	2.37*
T2Bd	0.031(1)	0.19674(4)	−0.19025(3)	0.0780(2)	2.37*
T3Ba	0.031(1)	−0.41414(5)	0.11949(5)	0.3776(4)	2.37*
T3Bb	0.031(1)	0.41414(5)	0.11949(5)	0.3776(4)	2.37*
T4Ba	0.031(1)	−0.08524(5)	−0.22445(5)	0.3721(4)	2.37*
T4Bb	0.031(1)	0.08524(5)	−0.22445(5)	0.3721(4)	2.37*
O1Ba	0.031(1)	−0.3764(1)	0.0893(1)	0.199(1)	2.37*
O1Bb	0.031(1)	−0.3764(1)	0.0893(1)	0.5525(9)	2.37*
O1Bc	0.031(1)	0.3764(1)	0.0893(1)	0.1989(9)	2.37*
O1Bd	0.031(1)	0.3764(1)	0.0893(1)	0.552(1)	2.37*
O2Ba	0.031(1)	−0.1228(1)	−0.1941(1)	0.195(1)	2.37*
O2Bb	0.031(1)	−0.1228(1)	−0.1941(1)	0.541(1)	2.37*
O2Bc	0.031(1)	0.1228(1)	−0.1941(1)	0.186(1)	2.37*
O2Bd	0.031(1)	0.1228(1)	−0.1941(1)	0.549(1)	2.37*
O3Ba	0.031(1)	−0.2366(1)	−0.1221(1)	0.640(1)	2.37*
O3Bb	0.031(1)	−0.2366(1)	−0.1221(1)	0.126(1)	2.37*
O3Bc	0.031(1)	0.2366(1)	0.1221(1)	0.621(1)	2.37*
O3Bd	0.031(1)	0.2366(1)	0.1221(1)	0.144(1)	2.37*
O4Ba	0.031(1)	0.4066(2)	0.1977(2)	0.377(2)	2.37*

(*continued on next page*)

Table 2 (*continued*)

Atom	Population	*x*	*y*	*z*	B_{eq} (Å^2)
O4Bb	0.031(1)	−0.4066(2)	0.1977(2)	0.377(2)	2.37*
O5Ba	0.031(1)	−0.1736(4)	−0.1930(3)	0.8736(9)	2.37*
O5Bb	0.031(1)	0.1683(4)	−0.1938(4)	−0.127(1)	2.37*
O6Ba	0.031(1)	−0.3262(2)	−0.0811(1)	0.3803(8)	2.37*
O6Bb	0.031(1)	0.3262(2)	−0.0811(1)	0.3803(8)	2.37*
O7Ba	0.031(1)	−0.2755(4)	−0.0003(3)	0.1279(9)	2.37*
O7Bb	0.031(1)	0.2749(4)	−0.0003(3)	0.1279(9)	2.37*
O8Ba	0.031(1)	−0.2557(4)	−0.2430(3)	0.1445(9)	2.37*
O8Bb	0.031(1)	0.2481(5)	0.2530(5)	0.613(1)	2.37*
O9B	0.031(1)	0.5029(4)	0.0976(2)	0.369(1)	2.37*
O10B	0.031(1)	−0.0012(5)	−0.2011(2)	0.375(1)	2.37*
NA1	0.08(1)	0.491(3)	0.004(3)	0.619(7)	3.3(12)*
NA2	0.25(1)	0.000(2)	−0.207(1)	0.394(5)	7.90*
NA3	0.12(1)	−0.016(3)	0.105(3)	0.835(7)	7.90*
NA4	0.17(2)	−0.012(3)	0.377(4)	0.895(7)	7.90*
NA5	0.07(4)	−0.007(3)	0.405(5)	0.851(5)	0.6(24)*
NA6	0.16(1)	0.002(3)	0.267(2)	0.832(5)	7.90*
NA7	0.15(2)	0.002(2)	0.162(2)	0.841(5)	6.0(13)*
W1	0.44(6)	−0.501(1)	0.065(3)	0.340(2)	4.9(5)
W2	0.48(2)	0.009(1)	0.088(1)	0.084(3)	7.90*
W3	0.28(2)	0.023(2)	0.092(2)	−0.285(5)	7.90*
W4	0.48(2)	−0.017(1)	0.322(1)	0.873(4)	7.90*
W5	0.31(2)	0.108(2)	0.014(9)	−0.969(4)	7.90*
W6	0.37(2)	−0.110(2)	−0.012(7)	0.557(4)	7.90*
S1	0.033(1)[a]	−0.1057(8)	0.0000(1)	0.175(1)	7.90*
C1a	0.033(1)[a]	−0.0484(7)	0.00000(4)	−0.007(1)	11.84*
C2a	0.033(1)[a]	−0.0484(7)	0.00000(7)	0.364(1)	11.84*
C3a	0.033(1)[a]	0.0272(7)	0.0000(2)	0.348(1)	11.84*
C4a	0.033(1)[a]	0.0331(8)	0.0000(2)	0.0173(1)	11.84*
N1a	0.033(1)[a]	0.0650(8)	0.0000(3)	0.173(1)	11.84*
C5a	0.033(1)[a]	0.0820(7)	0.0000(2)	−0.141(1)	11.84*
C6a	0.033(1)[a]	0.0533(5)	0.0000(2)	−0.306(1)	11.84*
C7a	0.033(1)[a]	−0.0271(7)	0.00000(4)	−0.330(1)	11.84*
C8a	0.033(1)[a]	−0.0765(7)	0.0000(1)	−0.174(1)	11.84*
N2a	0.033(1)[a]	−0.0533(4)	0.0000(1)	−0.495(2)	11.84*
C9a	0.033(1)[a]	−0.0816(5)	0.0000(2)	0.531(1)	11.84*
C10a	0.033(1)[a]	−0.0380(2)	0.0000(2)	0.683(2)	11.84*
C11a	0.033(1)[a]	0.0380(2)	0.0000(2)	0.666(2)	11.84*
C12a	0.033(1)[a]	0.0709(5)	0.0000(3)	0.500(1)	11.84*
N3a	0.033(1)[a]	−0.0689(5)	0.0000(2)	0.855(2)	11.84*
C13a	0.033(1)[a]	−0.1471(5)	0.0000(2)	0.903(2)	11.84*
C14a	0.033(1)[a]	−0.02207(8)	0.00000(4)	1.016(2)	11.84*
C15a	0.033(1)[a]	−0.133(1)	0.0000(2)	−0.528(4)	11.84*
C16a	0.033(1)[a]	−0.004(2)	0.0000(2)	−0.649(2)	11.84*
S1b	0.033(1)[a]	0.1016(7)	0.0025(3)	−0.411(1)	7.90*
C1b	0.033(1)[a]	0.0505(5)	−0.0137(2)	−0.222(1)	11.84*
C2b	0.033(1)[a]	0.0505(5)	−0.0274(3)	−0.593(1)	11.84*
C3b	0.033(1)[a]	−0.0168(5)	−0.0569(5)	−0.566(1)	11.84*
C4b	0.033(1)[a]	−0.0219(4)	−0.0472(4)	−0.2355(8)	11.84*
N1b	0.033(1)[a]	−0.0493(5)	−0.0650(5)	−0.3867(9)	11.84*
C5b	0.033(1)[a]	−0.0654(4)	−0.0610(5)	−0.0724(9)	11.84*
C6b	0.033(1)[a]	−0.0386(4)	−0.0428(5)	0.0878(7)	11.84*
C7b	0.033(1)[a]	0.0325(5)	−0.0100(3)	0.101(1)	11.84*
C8b	0.033(1)[a]	0.0766(7)	0.0041(3)	−0.060(1)	11.84*
N2b	0.033(1)[a]	0.0575(5)	0.0073(4)	0.261(1)	11.84*
C9b	0.033(1)[a]	0.0792(9)	−0.0207(4)	−0.762(1)	11.84*
C10b	0.033(1)[a]	0.0388(9)	−0.0444(5)	−0.907(1)	11.84*
C11b	0.033(1)[a]	−0.0284(7)	−0.0740(7)	−0.880(1)	11.84*
C12b	0.033(1)[a]	−0.0575(5)	−0.0813(8)	−0.710(1)	11.84*
N3b	0.033(1)[a]	0.0672(8)	−0.0379(5)	−1.081(1)	11.84*
C13b	0.033(1)[a]	0.1378(8)	−0.0077(7)	−1.133(3)	11.84*

Table 2 (*continued*)

Atom	Population	*x*	*y*	*z*	B_{eq} (Å^2)
C14b	0.033(1)[a]	0.0276(2)	−0.0617(8)	−1.239(2)	11.84*
C15b	0.033(1)[a]	0.1284(5)	0.0404(5)	0.282(3)	11.84*
C16b	0.033(1)[a]	0.0135(3)	−0.0068(1)	0.422(2)	11.84*

Coordinates with the same superscript were constrained to be equal. All atomic parameters (coordinates, population, isotropic displacement factors) labeled B are fully constrained and belong to a domain of mordenite shifted *c*/2 relative to the main part of the structure.

[a] Parameters of the MB-sites with the same superscript were constrained to be equal.

MB^+ molecule with its methyl groups at each end of the molecule and the molecular size of 7×16 Å (based on van der Waals radii) yields a slight compression of 12MRc along the *b*-axis. On the other hand the compressed 8-membered ring channel along *c* is slightly widened along the *b*-axis. This effect can also be envisioned by the ratio of the long axis to the short axis of the elliptic 12MRc and the compressed 8MRc. Taking the O7a–O7b distance (long axis) and the O10–O10 distance (short axis) in 12MRc, the ratio for mordenite-Na is 1.05, whereas for MB-mordenite-Na it is 1.1, expressing a more compressed ellipse. The long axis/short axis ratio for 8MRc is 1.53 for mordenite-Na, and 1.49 for MB-mordenite-Na.

The distribution of extra framework occupants (Na^+, H_2O) differs significantly from the corresponding distribution in mordenite-Na. Na cations in mordenite-Na are mainly concentrated on 4 sites (Fig. 4a); a highly occupied site (Na1) in the center of the compressed 8-membered channel along *c*, 3 less occupied sites within the 12-membered ring channel along *c* (Na2, Na3, Na4), where Na2 is positioned at the intersection to the 8-membered ring channel along *b*. Most surprisingly, the highly occupied Na1 in mordenite-Na is only low populated in MB-mordenite-Na. Furthermore, the Na population in the large 12MRc is reduced, and new, also low populated Na sites are found in 8MRb (Fig. 4b). The Na content determined in the structure refinement (4.02 Na per formula unit (pfu)) differs significantly from the analyzed Na content (5.52 Na pfu). This points to a strongly disordered Na distribution caused by the incorporation of MB^+, situated in the large 12-membered channel. By entering the large 12MRc, the bulky dye molecule displaces the channel occupants and shifts them partly to the connecting channel along *b*. Most H_2O molecules in the large 12MRc are missing, and only 6 H_2O are left (Fig. 4). Because of the strongly disordered distribution, it must be assumed that Na and H_2O sites cannot be clearly distinguished (similar scattering power, similar distance to the channel walls).

The two molecule sites localized in the 12-membered ring channel led to 0.26 MB^+ per formula unit. Thus, the chemical analysis of 0.28 MB^+ per formula unit (pfu) is in good agreement with the dye content determined in the structural refinement. 0.28 MB^+ pfu represents less than 30% loading of the mordenite channels. The periodicity of the mordenite *c* translation (7.5 Å) corresponds to nearly the half-length of the MB^+ molecule (16 Å). With two 12-membered ring channels per unit cell, this results in theoretical complete filling for 0.93 molecules per formula. The dye loading of less than 30% indicates a disordered molecule arrangement within the mordenite channels. This assumption is supported by the diffraction data where no diffuse scattering or superstructure reflections were detected.

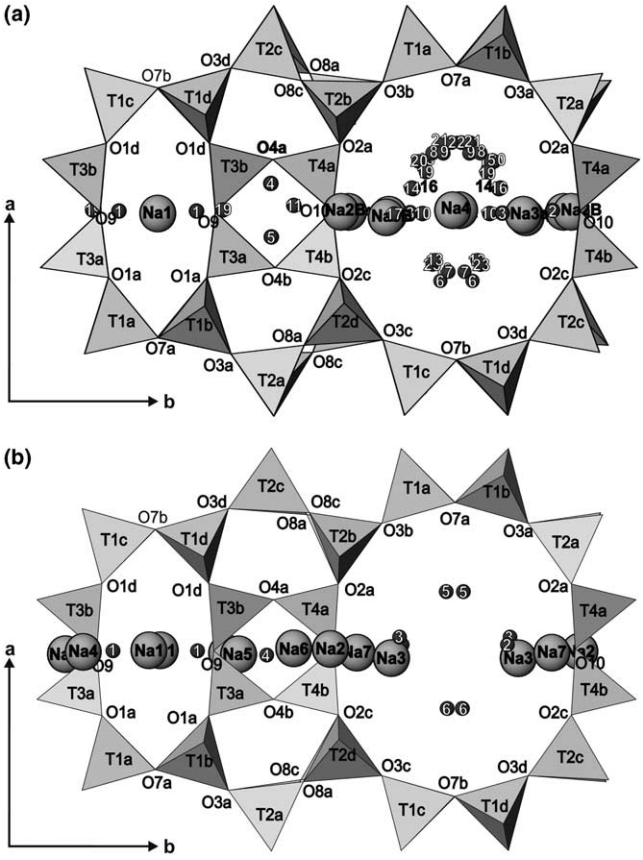

Fig. 4. (a) Tetrahedral framework and extra framework cations and H_2O molecules of mordenite-Na. (b) Tetrahedral framework and extra framework cations and H_2O molecules of MB-mordenite-Na. Black circles with white numbers are H_2O positions.

Although the structure refinement was performed in space group *Cc*, the mordenite framework exhibits topological symmetry *Cmcm* with a 2_1 axis passing through the center of the large 12MRc channels, a mirror plane

perpendicular to the crystal's *c*-axis and a mirror plane parallel to (1 0 0). On the first glance these requirements imposed by pseudo-symmetry do not agree with the results of the structure refinement where one MB^+ site is oriented upright and the other is opposite to the first one, shifted *c*/2, and slightly inclined to the 12MRc channel. The two resolved MB^+ sites are approximately related by a 2_1 axis. The missing symmetry equivalent positions (relative to the topological symmetry) should not be taken as proof for an acentric MB^+ arrangement within a pseudo-centrosymmetric channel environment. We consider this as an artifact caused by severe correlations in the diffraction data due to a low symmetry refinement (*Cc*) of a structure with high topological symmetry (*Cmcm*). If four fully constrained MB^+ molecules are introduced in the 12MRc channels according to the topological symmetry, the populations of these molecules are highly correlated and cannot simultaneously be refined. Therefore the populations of the two refined molecules were constrained to be equal. In other words, we cannot distinguish centrosymmetric and acentric MB^+ arrangement. The most appropriate interpretation of the MB^+ distribution based on our diffraction data is as following. The inner surface of the mordenite 12MRc channels exhibits preferred positions for the attachment of MB^+ (Fig. 5). This means that the mordenite channels cannot be filled by continuous stacks of MB^+ along *c* where the MB^+ separation would be dictated by van der Waals contacts. Such an hypothetical arrangement would probably be incommensurate with the available docking sites on the channel surface. Because the topological symmetry requires that the preferred MB^+ sites are separated by *c*/2 one may assume from Fig. 5 that two closely spaced MB^+ molecules find space in four translations of the host structure along *c* if the adjacent molecules are rotated 180° around the channel axis to prevent short intermolecular contacts. One should also consider that the two resolved MB^+ sites in the structure refinement were obtained by very rigid constraints concerning interatomic distances and isotropic displacement parameters. Thus we question whether the resolved molecule positions are actually two independent sites or rather an indication of severe librational disorder of the up-right orientation with continuous variations.

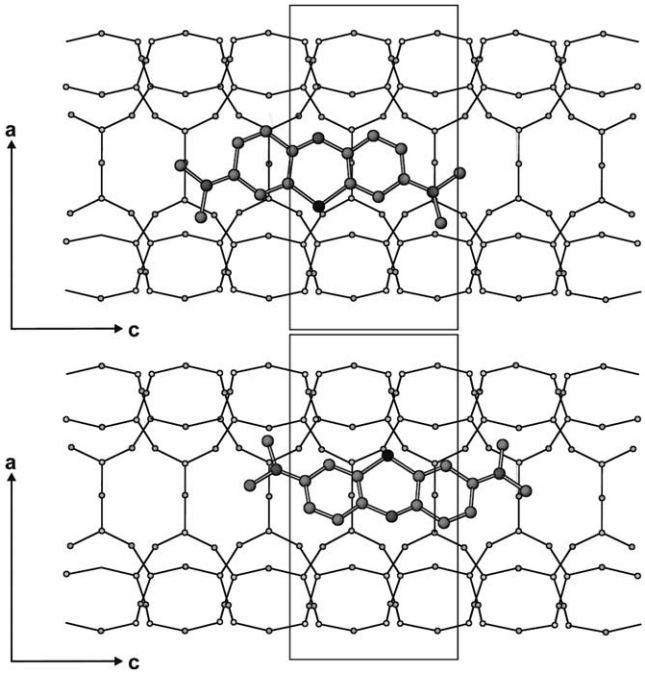

Fig. 5. MB^+ molecule sites within the large 12-membered ring channel along *c*. Unit cell dimensions are indicated by a square. Black dots represent the sulfur-atom. One molecule is shifted approximately *c*/2 to another.

Shortest S···O, N···O and C···O distances from the MB^+ molecules to the mordenite framework are summarized in Table 3. Compared with literature data, where C···O distances of 2.8–3.3 Å [16,30] are reported, the C···O distances (2.83–3.02 Å) in this study are relatively short, indicating CH···O hydrogen bonding from the molecules to the mordenite framework. Calculated hypothetical H-atom coordinates using CH_3 and CH constrains resulted in CH···O distances around 2.12 Å with C–H–O angles of 145° for the shortest contacts to the mordenite framework, e.g. for the C15b–H–O7a group. These calculated H sites were not included in the refinement.

Partial demethylation of MB^+ to the neutral trimethylthionin (removal of a CH_3 group) has been reported at high pH and high temperature [31], and was also postulated in an X-ray powder diffraction experiment on MB^+ modified NaY [11], where the sample was heated to 200 °C. Although in our study, MB^+ was incorporated at 90 °C, it can be assumed that MB is not present as neutral demethylated TMT. The demethylation of MB^+ to TMT is described as a base catalyzed reaction of MB^+ at the surface of denitrated zeolite NaA–Na_2O [31]. If TMT were present in the ion-exchange solution, it would not be incorporated because of its neutral state. The conversion of MB^+ to TMT within the mordenite channels can also be ruled out because of charge balance reasons. Furthermore the expansion of the unit cell along the *a*-axis also points to the incorporation of MB^+ with methyl groups at both end of the molecule.

Table 3
Shortest S···O, C···O and N···O distances from the MB molecule to the channel wall oxygens

Molecule 1		Molecule 2	
S1a-O7b	3.09(1) Å	S1b-O7a	3.17(1) Å
N1a-O7a	3.84(1) Å	N1b-O2c	2.99(1) Å
C13a-O7b	2.86(1) Å	C15b-O7a	3.02(1) Å
C16a-O7b	2.83(2) Å	C15b-O3b	2.83(1) Å

Using diffuse reflectance spectroscopy, Zanjanchi and Sohrabnejad [6] observed two bands at 660 nm and 610 nm, which they assigned to monomeric and dimeric species of MB^+ within the mordenite channels. It was shown that dyes form H-dimers (stacked) or J-dimers (slanted stacked) [32]. The existence of dimeric methylene blue in the mordenite channels cannot be confirmed by this study. Due to steric reasons a dimeric arrangement (stacked H-dimer or slanted stacked J-dimer) cannot be realized, and methylene blue molecules are only present as monomers. It must be assumed that the absorption band found at 610 nm [6], which was attributed to dimers within the channels, belongs to MB dimers on the surface of mordenite.

In spite of comparable channel openings of mordenite (6.5×7 Å) and zeolite L (7.1 Å), the incorporation of MB^+ into zeolite L failed [12]. It seems that the mordenite framework with its oblate channel shape is more flexible for the incorporation of large dye molecules than the zeolite L framework with its circular shaped channels. Evidence of the higher flexibility is the more elliptical channel cross-section after incorporation of MB^+. In addition, one may assume that the relatively mobile and monovalent Na as extra framework cation may also favour the incorporation of MB^+ into the zeolite channels. MB^+ was incorporated in zeolites with Na^+ as an extra framework cation, but it failed for zeolites with Ca^{2+} and K^+ as an extra framework cation [6,12].

It was shown in this study that MB^+ can be incorporated into large mordenite single-crystals, where MB^+ molecules exist as monomers in the larger 12-membered ring channels. The close fit of the molecule results in short contacts to the mordenite framework. The experimental location of the molecule is simplified in two ways, (1) the close fit of the molecule reduces the rotational disorder of the molecule within the channel, (2) the position of the molecule can easily be defined by the heavy scattering atoms as sulphur. It was demonstrated that single-crystal X-ray diffraction is an ideal probe for the characterization of arrangement and bonding of a dye molecule encapsulated in a zeolite framework.

Acknowledgement

This study was supported by the Swiss 'Nationalfond', credit 20-65084.01 to T. Armbruster. P. Simoncic thanks the International Center for Diffraction Data (ICDD) for a 2004 Ludo Frevel Crystallography Scholarship. We acknowledge the European Synchrotron Radiation Facility for provision of synchrotron radiation facilities and we would like to thank V. Dmitriev for assistance in using the Swiss-Norwegian Beam line 1A. Furthermore, we would like to thank Prof. Gion Calzaferri for the inspiring ideas and helpful suggestions. We thank Stefan Huber and Olivia Bossart for help with the fluorescence microscope.

References

[1] G. Calzaferri, S. Huber, H. Maas, C. Minkowski, Angew. Chem. Int. Ed. 42 (32) (2003) 3732.
[2] D. Cox, T.E. Gier, G.D. Stucky, Solid State Ion. 32/33 (1990) 514.
[3] M. Ehrl, F.W. Deeg, C. Bräuchle, O. Franke, A. Sobbi, G. Schulz-Ekloff, D. Wöhrle, J. Phys. Chem. 98 (1994) 47.
[4] R. Hoppe, G. Schulz-Ekloff, D. Wöhrle, M. Ehrl, C. Bräuchle, in: P.A. Jacobs, N.I. Jaeger, L. Kubelkova, B. Wichterlova (Eds.), Zeolite Chemistry and Catalysis, Elsevier, Amsterdam, 1991.
[5] M. Arvand, Sh. Sohrabnezhad, M.F. Mousavi, M. Shamsipur, M.A. Zanjanchi, Anal. Chim. Acta 491 (2003) 193.
[6] M.A. Zanjanchi, Sh. Sohrabnejad, J. Inclus. Phen. Macroc. Chem. 46 (2003) 43.
[7] M.G. Neumann, I.A. Pastre, Solar Energy 38 (6) (1987) 431.
[8] S.E. Jayaraj, M. Umadevi, V. Ramakrishnan, J. Inclus. Phen. Macroc. Chem. 40 (2001) 203.
[9] R. Hoppe, G. Schulz-Ekloff, D. Wöhrle, E.S. Shpiro, O.P. Tkachenko, Zeolites 13 (1993) 222.
[10] R. Hoppe, G. Schulz-Ekloff, D. Wöhrle, C. Kirschhock, H. Fuess, Langmuir 10 (1994) 1517.
[11] R. Hoppe, G. Schulz-Ekloff, D. Wöhrle, C. Kirschhock, H. Fuess, L. Uytterhoeven, R. Schoonheydt, Adv. Mater. 7 (1) (1995) 61.
[12] G. Calzaferri, N. Gfeller, J. Phys. Chem. 96 (1992) 3428.
[13] W.M. Meier, Zeit. Kristall. 115 (1961) 439.
[14] W.M. Meier, in: L.B. Sand, F.A. Mumpton (Eds.), Natural Zeolites, Occurrence, Properties, Use, 1978, p. 99.
[15] T. Armbruster, M.E. Gunter, in: D.L. Bish, D.W. Ming (Eds.), Reviews in Mineralogy & Geochemistry, Vol. 45, Natural Zeolites: Occurrence, Properties, Use, 2002, p. 1.
[16] B. Hennessy, S. Megelski, C. Marcolli, V. Shklover, C. Bärlocher, G. Calzaferri, J. Phys. Chem. B 103 (1999) 3340.
[17] S. Megelski, A. Lieb, M. Pauchard, A. Drechsler, S. Glaus, C. Debus, A.J. Meixner, G. Calzaferri, J. Phys. Chem. B 105 (2001) 25.
[18] J. Warzywoda, A.G. Dixon, R.W. Thompson, A. Sacco Jr., J. Mater. Chem. 5 (7) (1995) 1019.
[19] P. Simoncic, T. Armbruster, Am. Miner. 89 (2004) 421.
[20] P. Simoncic, T. Armbruster, Micropor. Mesopor. Mater. 71 (2004) 185.
[21] P. Simoncic, T. Armbruster, Zeolite '02, in: P. Misaelides (Ed.), 6th International Conference on the Occurrence, Properties and Utilization of Natural Zeolites, 2002, p. 336.
[22] Oxford Diffraction (2001) Xcalibur System, User Manual, CrysAlis Software Package. Version 1.169. Oxfordshire, UK.
[23] G.M. Sheldrick, SADABS, Version 2.06, Empirical Absorption Correction Program, University of Göttingen, Germany, 2002.
[24] G.M. Sheldrick, SHELX-97, University of Göttingen, Germany, 1997.
[25] A. Alberti, P. Davoli, P.G. Vezzalini, Zeit. Kristall. 175 (1986) 249.
[26] R. Gramlich-Meier, Strukturparameter in Zeolithen der Mordenitfamilie, Dissertation ETH Zürich, Nr. 6760, 1981.
[27] H.E. Marr III, J.M. Stewart, Acta Cryst. B 29 (1973) 847.
[28] Advanced Chemistry Development Inc.; ChemSketch (2001) Ontario, Canada.
[29] P. Simoncic, Incorporation of Guest-Molecules into Zeolite Mordenite, PhD Thesis, University of Bern, 2004.
[30] H. van Koningsveld, F. Tuinstra, H. van Bekkum, J.C. Jansen, Acta Cryst. B 45 (1989) 423.
[31] M. Susic, N. Petranovic, B. Miocinovic, J. Inorg. Nucl. Chem. 34 (1972) 2349.
[32] W. West, S. Pearce, J. Phys. Chem. 69 (9) (1965) 1894.